Materials Science and Engineering C 33 (2013) 3931–3934

Contents lists available at ScienceDirect

Materials Science and Engineering C

journal homepage: www.elsevier.com/locate/msec

Fabrication and characterization of a zirconia/multi-walled carbon nanotube mesoporous composite

Zonghua Wang [a,*], Jianfei Xia [a], Yanzhi Xia [a,**], Caiyu Lu [a], Guoyu Shi [a], Feifei Zhang [a], Fuqiang Zhu [a], Yanhui Li [a], Linhua Xia [a], Jie Tang [b]

[a] Laboratory of Fiber Materials and Modern Textile, the Growing Base for State Key Laboratory, College of Chemical and Environment Engineering, Qingdao University, Shandong 266071, PR China
[b] National Institute for Materials Science, Sengen 1-2-1, Tsukuba 305-0047, Japan

ARTICLE INFO

Article history:
Received 28 August 2012
Received in revised form 9 April 2013
Accepted 13 May 2013
Available online 22 May 2013

Keywords:
ZrO_2
MWCNTs
CTAB
Mesoporous–nanotube
Composite

ABSTRACT

A zirconia/multi-walled carbon nanotube (ZrO_2/MWCNT) mesoporous composite was fabricated via a simple method using a hydrothermal process with the aid of the cationic surfactant cetyltrimethylammonium bromide (CTAB). Transmission electron microscopy (TEM), N_2 adsorption–desorption, Fourier transform infrared spectroscopy (FT-IR) and X-ray diffraction (XRD) techniques were used to characterize the as-made samples. The cubic ZrO_2 nanocrystallites were observed to overlay the surface of MWCNTs, which resulted in the formation of a novel mesoporous–nanotube composite. On the basis of a TEM analysis of the products from controlled experiment, the role of the acid-treated MWCNTs and CTAB was proposed to explain the formation of the mesoporous–nanotube structure. The as-made composite possessed novel properties, such as a high surface area (312 $m^2 \cdot g^{-1}$) and a bimodal mesoporous structure (3.18 nm and 12.4 nm). It was concluded that this composite has important application value due to its one-dimensional hollow structure, excellent electric conductivity and large surface area.

1. Introduction

Since the first report of silica-based mesoporous materials (M41S) in 1992 [1,2], mesoporous materials have attracted great interest in different areas of science because of their high surface area, narrow pore size distribution and large pore volume. Recently, many efforts have been focused on the synthesis of transition metal oxides with mesoporous structure due to their excellent catalytic, optical and electronic characteristics [3–5]. The well-developed mesoporous transition-metal oxides materials, which are synthesized through various surfactant-templated hydrothermal methods or modified sol–gel processes, have been extensively exploited in the past few years [6–11].

Carbon nanotubes (CNTs), as a new form of carbon nanomaterials with their unique electrical properties, high chemical stability and high surface-to-volume ratio, have been considered as a powerful reinforcement of transition-metal oxides to improve their electrical conductivity and mechanical and thermal properties [12–14]. Among the transition-metal oxides, there was particularly intensive focus on ZrO_2 because of its unique properties such as its high ion-exchange capacity and higher redox activity and selectivity [15–18], which made it an attractive material for applications in separation, catalysis and sensors. ZrO_2 has three polymorphs: monoclinic (m-phase, below 1170 °C), tetragonal (t-phase, between 1170 and 2370 °C) and cubic (c-phase, above 2370 °C) [19]. The cubic ZrO_2 possesses much better mechanical properties and ionic conductivity, but it is difficult to obtain because reactions towards ZrO_2 typically lead to the formation of mixed phases [20].

There has been growing concern about functionalizing mesoporousmaterials with nanostructured carbon. Moriguchi and coworkers successfully synthesized CNT-containing mesoporous TiO_2 with a bicontinuous microemulsion-aided process [21]. Du and coworkers have successfully prepared a hierarchically ordered porous TiO_2-graphene composite via a confinement self-assembly method [22]. To the best of our knowledge, there have been few reports about ZrO_2-loaded CNTs, and most of the as-made composites are nonporous [23–26]. In this work, a new mesoporous–nanotube composite (ZrO_2/MWCNT) was fabricated with the aid of one type of cationic surfactant (cetyltrimethylammonium bromide, CTAB) via a hydrothermal process. The preparation and structural properties of the composite were investigated in detail.

2. Experimental

2.1. Reagents

Spaghetti-like multi-wall carbon nanotubes (MWCNTs) with an external diameter of 10 nm prepared by the CVD method, purity > 95%,

* Correspondence to: Z. Wang, Department of Chemistry, College of Chemistry, Chemical Engineering and Environment, Qingdao University, Qingdao 266071, China. Tel./fax: +86 532 85950873 (O), +86 13853219173 (mobile).
** Correspondence to: Y. Xia, Department of Chemistry, College of Chemistry, Chemical Engineering and Environment, Qingdao University, Qingdao 266071, China.
E-mail addresses: wang_zonghua@yahoo.com.cn (Z. Wang), qdxyzh@163.com (Y. Xia).

0928-4931/$ – see front matter © 2013 Elsevier B.V. All rights reserved.
http://dx.doi.org/10.1016/j.msec.2013.05.031

were provided by Prof. Fan's research group (Physics Department, Tsinghua University, Beijing, China) [27]. Zirconium oxychloride ($ZrOCl_2 \cdot 8H_2O$) was purchased from Tianjin Bodi Chemical Holding Co., Ltd. CTAB was purchased from Shanghai Aibi Chemistry Preparation Co., Ltd. The other reagents used were all of analytical grade, and doubly distilled water was used.

2.2. Fabrication of the ZrO_2/MWCNT composite

MWCNTs were treated with mixture of concentrated sulfuric acid and nitric acid (3:1, v/v) under ultrasonication for 10 h, followed by an extensive washing with doubly distilled water to pH = 7 and then drying at 60 °C before use. Fifty milligrams of acid-treated MWCNTs and 20 mg of CTAB were dispersed into 30 mL of doubly distilled water. The preparation process was conducted as follows: I) The mixture was sonicated for 2 h to form a stable suspension. II) Then, 1 mL of 2 M NaOH was immediately added into the suspension under stirring. III) Next, 45 mg of $ZrOCl_2$ were slowly added to the mixture above with vigorous agitation. IV) The mixture was then transferred into a stainless steel Teflon-lined autoclave of 50 mL in capacity and maintained for 15 h at 150 °C. V) The products obtained were centrifuged and washed six times with ethanol to remove CTAB. The final products were denoted as ZrO_2/MWCNTs.

For comparison, a sample denoted as ZrO_2/MWCNTs-1 was prepared following the I–V procedures using 50 mg of original MWCNTs and 20 mg of CTAB as the starting materials, and another sample denoted as ZrO_2/MWCNTs-2 was prepared following the I–V procedures using 50 mg of acid-treated MWCNTs as the starting material in the absence of CTAB.

2.3. Apparatus and measurements

TEM images were obtained on a JEOL JEM 1200FX II at an accelerating voltage of 100 kV. A high-resolution transmission electron microscopy (HRTEM) image was taken on a JEM2010F at an accelerating voltage of 120 kV. XRD patterns were obtained on a Philips X'Pert MPD diffractometer equipped with Cu Ká radiation (ë = 1.5406 Å). FT-IR spectra on pellets of the samples with KBr were recorded on a Nicolet5700 spectrometer (Nicolet, USA). N_2 adsorption–desorption analysis was performed at 77 K on a Micromeritics TriStar 3000 apparatus. The surface area was determined using the BET equation.The pore volume and the pore size distribution were calculated from the desorption branch of the N_2 adsorption isotherm using the Barrett–Joyner–Halenda (BJH) formula.

3. Results and discussion

3.1. Characterization of the ZrO_2/MWCNT composite

Fig. 1(a) shows the TEM image of ZrO_2/MWCNTs-1 obtained using the original MWCNTs as the starting material. The MWCNTs and the ZrO_2 nanoparticles are separated from each other. Fig. 1(b) shows the general morphology of the ZrO_2/MWCNTs. We can observe that the ZrO_2 nanoparticles are attached to the acid-treated MWCNTs. It is assumed that the active groups (such as carboxyl and hydroxyl) on the surface of the acid-treated MWCNTs played an important role for the attachment of ZrO_2. In addition, the acid-treated MWCNTs have a higher zeta potential value (−47.6 mV), which can prevent the treated CNTs from aggregating and thereby stabilize the suspension. These results are consistent with results reported in the literature [28]. Furthermore, the good dispersal stability can be maintained for 2 weeks at least, which is useful for making ZrO_2 effectively supported on CNTs. The selected area electron diffraction (SAED) analysis of ZrO_2/MWCNTs is shown in Fig. 1(c). The polycrystalline rings ascribed to the (111), (200), (220) and (311) were observed, which proved that the ZrO_2 attached to the MWCNTs had a cubic phase polycrystalline structure. Fig. 1(d) shows the HRTEM image from the representative pores of the composite, from which we can observe a well-defined lattice fringe, revealing that the wall structure of ZrO_2 attached to the MWCNTs was very crystalline. The mesoporous ZrO_2 was assumed to be formed by the organization of inorganic precursors around CTAB under hydrothermal conditions, and the pores were formed after removing the CTAB. The porous structure was formed during the process of ZrO_2 nanocrystallite growth. This result is similar to a previous report [29].

3.2. N_2 adsorption–desorption curves

The N_2 adsorption–desorption isotherm curves of the composites ZrO_2/MWCNTs-2 and ZrO_2/MWCNTs are shown in Fig. 2. Curve a shows a reversible type II isotherm, which is the normal form of an isotherm obtained with a non-porous or macroporous adsorbent according to the IUPAC nomenclature. The beginning of the almost linear middle section of the isotherm indicates the stage at which monolayer coverage is complete. It was suggested that the ZrO_2/MWCNTs-2 composite prepared without CTAB is macroporous or nonporous solid. Curve b exhibited the type IV isotherms with a distinct hysteresis loop at the relative pressure of $P/P0$. According to the IUPAC nomenclature, this curve is a characteristic of the different processes between adsorption

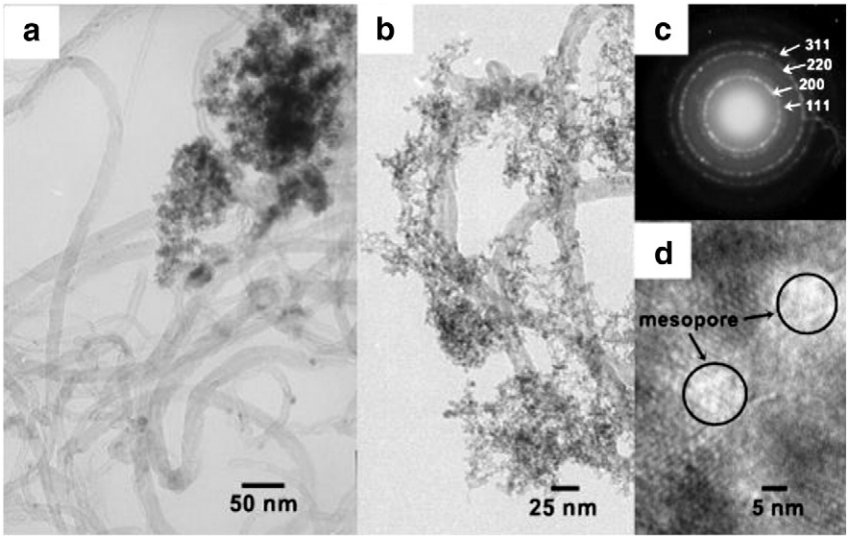

Fig. 1. TEM images of ZrO_2/MWCNTs-1 (a), ZrO_2/MWCNTs (b); SAED pattern of ZrO_2/MWCNTs (c); HRTEM of ZrO_2/MWCNTs (d).

into and desorption from the mesopores. The result confirmed the mesoporous structure of the ZrO_2/MWCNTs.

Pore size distributions of the samples were investigated by using the BJH (Barrett-Joyner-Halenda) model shown in Fig. 3. The pore parameters of the samples were calculated by N_2 adsorption-desorption isotherms. The pore size of ZrO_2/MWCNTs-2 showed a broad distribution (Fig. 3. curve b), revealing bigger agglomerates which leads to a broader pore distribution. ZrO_2/MWCNTs-2 was prepared in the absence of CTAB, which acts as a porogenic agent. In the preparation process, products with a mesoporous structure were assumed to be formed by the organization of inorganic precursors around CTAB under hydrothermal conditions. Thus, ZrO_2/MWCNTs-2 was a macroporous or nonporous solid, and the pore size showed a broad distribution. The pore sizes of the ZrO_2/MWCNTs were centered at 3.18 nm and 12.4 nm (Fig. 3. curve a). The pores centered at 3.18 nm are the MWCNTs inner cavities, close to the inner diameter of MWCNTs [30]. The pores centered at 12.4 nm mainly come from the aggregated ZrO_2 nanocrystallites, which is consistent with the HRTEM analysis. Such porous materials with the bimodal pore size distribution are important and useful for catalysis because the small pores can contribute to a large area of the active surface for the strong interaction of adsorbed molecules with the active sites, whereas the large pores can provide channels for fast intraparticle molecular transfer [31]. Furthermore, the specific surface area of ZrO_2/MWCNTs is 312 $m^2 \cdot g^{-1}$ while that of the ZrO_2/MWCNTs-2 is 110 $m^2 \cdot g^{-1}$. The pore volume of ZrO_2/MWCNTs is 0.74 cm^3/g while that of ZrO_2/MWCNTs-2 is 0.39 cm^3/g. The results indicate that a mesoporous structure was generated with the aid of CTAB.

According to the TEM analysis and the N_2 adsorption–desorption analysis, it was concluded that the active groups (such as carboxyl and hydroxyl) of the MWCNTs surface and CTAB were necessary for the formation of ZrO_2/MWCNTs. According to Wen's work [32], the charge density matching between the inorganic species and the surfactants is very important for the formation of organic–inorganic mesophases. In this work, we used $ZrOCl_2 \cdot 8H_2O$ and CTAB as inorganic precursors and porogenic agents, respectively. On one hand, electronegative groups such as carboxyl and hydroxylpresent on MWCNTs could absorb positive CTA^+ micelles on the surface of the MWCNTs via electrostatic interactions. On the other hand, due to hydrogen bonding interactions and electrostatic interactions, the micelles CTA^+ were surrounded by OH^- after sodium hydroxide was added. Afterward, the added Zr^{4+} ions reacted with OH^- at the interface of the micelles and formed ZrO_2 crystallites attached to the MWCNTs after the hydrothermal treatment and surfactant removal.

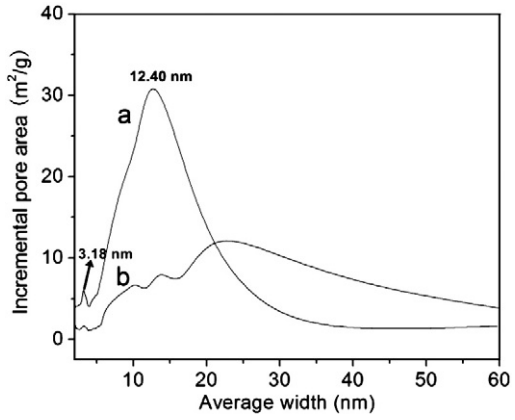

Fig. 3. Pore size distribution of ZrO_2/MWCNTs (a) and ZrO_2/MWCNTs-2 (b).

3.3. FT-IR spectra and XRD patterns

To consider the effect of ethanol on the removal of CTAB, the FT-IR spectra of ZrO_2/MWCNT mesoporous composites before (Fig. 4. curve a) and after (Fig. 4. curve b) washing with ethanol are shown. The broad band at approximately 3400 cm^{-1} can be attributed to –OH groups and physically adsorbed water, suggesting that the composite is hydrophilic in nature. Compared with curve a, the absence of the bands at 2870 and 2950 cm^{-1} was shown in curve b, which can be assigned to the $-CH_2$ group from CTAB, confirming that most of the CTAB was successfully removed after washed with ethanol.

The XRD patterns of ZrO_2/MWCNTs and MWCNTs are shown in Fig. 5. The most intense peak of MWCNTs at 26.17° corresponds to the (002) plane, which reflects the crystallinity of the MWCNTs in Fig. 5 curve a. The peaks at 30.23°(111), 35.22°(200), 50.51°(220), 59.91°(311), 62.97°(222) and 74.05°(400) of the ZrO_2/MWCNT composite (Fig. 5. curve b) clearly represent the formation of cubic ZrO_2 (JCPDS, CAS number 27–0997) crystallites, which is consistent with the SAED analysis. No obvious peaks corresponding to other phases of ZrO_2 were observed in curve b. The characteristic peak of MWCNTs (002) was significantly weakened, which mainly results from the coverage with ZrO_2. The well-resolved diffraction results confirm that ZrO_2/MWCNTs area composite of cubic ZrO_2 and MWCNTs.

Most of the previously reported mesoporous ZrO_2 do not show such a pure cubic phase [10–15,33,34], which generally exists as a stable form of ZrO_2 crystals at high temperatures (above 2370 °C) [35]. Previous studies indicated that the addition of CNTs or carbon

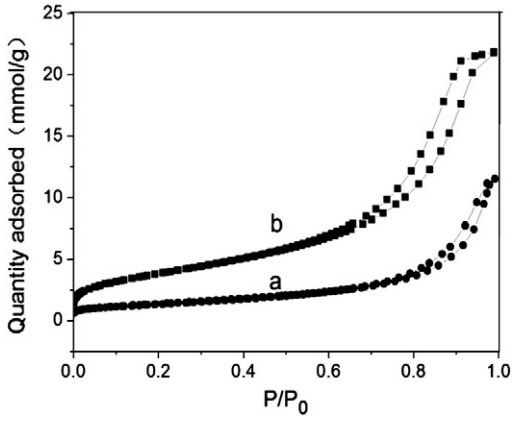

Fig. 2. N_2 adsorption–desorption isotherm curves of ZrO_2/MWCNTs-2 (a) and ZrO_2/MWCNTs (b).

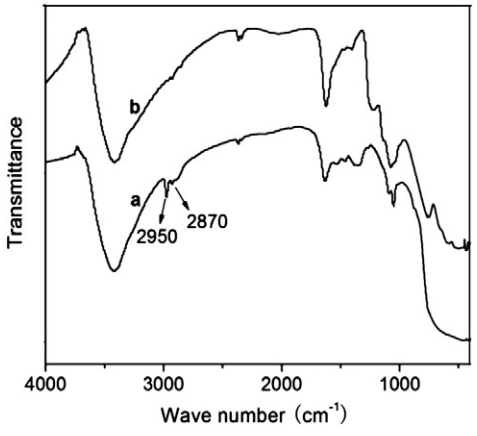

Fig. 4. FT-IR spectra of the ZrO_2/MWCNT mesoporous composite before (a) and after (b) washing with ethanol.

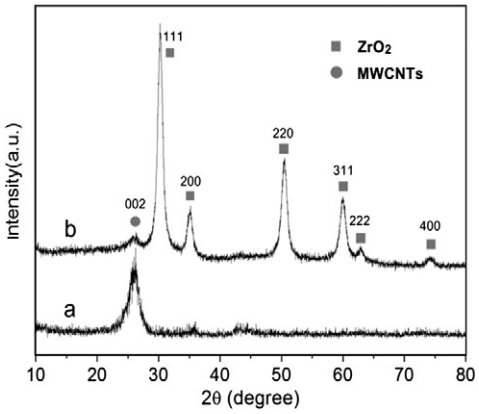

Fig. 5. XRD patterns of MWCNTs (a) and ZrO_2/MWCNTs (b).

powders tended to stabilize cubic ZrO_2 at room temperature [36,37] because CNTs not only provide large nano-scale nuclear sites for ZrO_2 but also prevent ZrO_2 particles from aggregating and growing in the drying process, both of which are propitious for the stabilization of the cubic phase. Our result indicated that the structure of ZrO_2 was stabilized as a cubic phase with MWCNTs at room temperature.

4. Conclusions

In conclusion, we present a facile method to fabricate a ZrO_2/MWCNT mesoporous composite via an easy, efficient hydrothermal process with the aid of the cationic surfactant CTAB. A possible mechanism was proposed to explain the formation of the mesoporous–nanotube structure. Acid-treated MWCNTs were favorable for the stabilization of cubic ZrO_2; the active groups (carboxyl and hydroxyl) of the MWCNTs and CTAB played an important role in forming the mesoporous–nanotube composite.These results indicated that the cubic ZrO_2 nanocrystallites could be attached to the outside surface of the MWCNTs. This composite possessed novel properties, such as a high surface area (312 $m^2 \cdot g^{-1}$) and a bimodal mesoporous structure (3.18 nm and 12.4 nm). Additionally, this mesoporous–nanotube structure not only can acquire a high surface area and a bimodal mesoporous and one-dimension structure but can also enhance the electrical conductivity with the combination of conductive CNTs. The composite can potentially be used as a catalyst, a sensor, an ideal starting material for sintered ceramics and an ideal reinforcement in other composites. The fabrication method is expected to extend the palette of available methods for the growth and assembly of different mesoporous materials-tube composites, which anticipates and encourages the extensive applications of these novel materials.

Acknowledgments

This work was financially supported by National Natural Science Foundation of China (authorized number: 20975056, 21275082 and 81102411), the Natural Science Foundation of Shandong (ZR2011BZ004 and ZR2011BQ005), JSPS and NSFC under the Japan–China Scientific Cooperation Program (21111140014), the State Key Laboratory of Analytical Chemistry for Life Science (SKLACLS1110) and the National Key Basic Research Development Program of China (973 special preliminary study plan, Grant no.: 2012CB722705).

References

[1] C.T. Kresge, C.T. Kresge, M.Z. Leonowicz, W.J. Roth, J.C. Vartuli, J.S. Beck, Nature 359 (1992) 710–712.
[2] J.S. Beck, J.C. Vartuli, W.J. Roth, M.Z. Leonowicz, C.T. Kresge, K.T. Schmitt, C.T.W. Chu, D.H. Olson, E.W. Sheppard, J. Am. Chem. Soc. 114 (1992) 10834–10843.
[3] M.J. Rozenberg, M.J. Sánchez, R. Weht, C. Acha, F. Gomez-Marlasca, P. Levy, Phys. Rev. B 81 (2010) 115101–115105.
[4] S. Balaji, Y. Djaoued, A.S. Albert, R.Z. Ferguson, R. Bruning, B.L. Su, J. Mater. Sci. 44 (2009) 6608–6616.
[5] J.H. Wang, J. Kim, E. Ramasamy, W. Choi, J. Lee, Microporous Mesoporous Mater. 143 (2011) 149–156.
[6] G. Pacheco, E. Zhao, E.D. Valdes, A. Garcia, J.J. Fripiat, Microporous Mesoporous Mater. 32 (1999) 175–188.
[7] X.M. Liu, G.Q. Lu, Z.F. Yan, J. Phys. Chem. B 108 (2004) 15523–15528.
[8] M. Rezaei, S.M. Alavi, S. Sahebdelfar, X.M. Liu, Z.F. Yan, J. Mater. Sci. 42 (2007) 7086–7092.
[9] Z.Q. Zhao, D.R. Chen, X.L. Jiao, J. Phys. Chem. C 111 (2007) 18738–18743.
[10] H. Zhang, D.D. Wang, L.E. Deng, Z.T. An, Q. Tang, Y.S. Wang, W.C. Li, Mater. Charact. 59 (2008) 493–497.
[11] J. Konishi, K. Fujita, S. Oiwa, K. Nakanishi, K. Hirao, Chem. Mater. 20 (2008) 2165–2173.
[12] P.C. Chen, G.A. Shen, Y. Shi, H.T. Chen, C.W. Zhou, ACS Nano 4 (2010) 4403–4411.
[13] K. Byrappa, A.S. Dayananda, C.P. Sajan, B. Basavalingu, M.B. Shayan, K. Soga, M. Yoshimura, J. Mater. Sci. 43 (2008) 2348–2355.
[14] K. Pal, D.J. Kang, Z.X. Zhang, J.K. Kim, Langmuir 26 (2010) 3609–3614.
[15] T. Andersen, Q.N.T. Nguyen, R. Trones, T. Greibrokk, J. Chromatogr. A 1018 (2003) 7–18.
[16] V. Idakiev, T. Tabakova, A. Naydenov, Z.Y. Yuan, B.L. Su, Appl. Catal. A Gen. 63 (2006) 178–186.
[17] B. Liu, Y. Cao, D.D. Chen, J.L. Kong, J.Q. Deng, Anal. Chim. Acta 478 (2003) 59–66.
[18] Q. Yuan, Y. Liu, L.L. Li, Z.X. Li, C.J. Fang, W.T. Duan, X.G. Li, C.H. Yan, Microporous Mesoporous Mater. 124 (2009) 169–178.
[19] F. Lupo, R. Kamalakaran, C. Scheu, N. Grobert, M. Ruhle, Carbon 42 (2004) 1995–1999.
[20] M.N. Tahir, L. Gorgishvili, J.X. Li, T. Gorelik, U. Kolb, L. Nasdala, W. Tremel, Solid State Sci. 9 (2007) 1105–1109.
[21] I. Moriguchi, R. Hidaka, H. Yamada, T. Kudo, H. Murakami, N. Nakashima, Adv. Mater. 18 (2006) 69–73.
[22] J. Du, X.Y. Lai, N.L. Yang, J. Zhai, D. Kisailus, F.B. Su, D. Wang, L. Jiang, ACS Nano 5 (2011) 590–596.
[23] A. Duszova, J. Dusza, K. Tomasek, G. Blugan, J. Kuebler, J. Eur. Ceram. Soc. 28 (2008) 1023–1027.
[24] H.Q. Song, X.P. Qiu, F.S. Li, Appl. Catal. A Gen. 364 (2009) 1–7.
[25] Z.Y. Sun, X.R. Zhang, N. Na, Z.M. Liu, B.X. Han, G.M. An, J. Phys. Chem. B 110 (2006) 13410–13414.
[26] R.P. Liang, M.Q. Deng, S.G. Cui, H. Chen, J.D. Qiu, Mater. Res. Bull. 45 (2010) 1855–1860.
[27] Z.H. Wang, S.F. Xiao, Y. Chen, J. Electroanal. Chem. 589 (2006) 237–242.
[28] M.W. Shen, S.H. Wang, X.Y. Shi, X.S. Chen, Q.G. Huang, E.J. Petersen, R.A. Pinto, J.R. Baker, W.J. Weber, J. Phys. Chem. C 113 (2009) 3150–3156.
[29] P. Trens, M.J. Hudson, R. Denoyel, J. Mater. Chem. 8 (1998) 2147–2152.
[30] C. Lu, H. Chiu, Eng. Sci. 61 (2006) 1138–1145.
[31] L. Zhang, Q. Zhang, J.H. Li, Chem. Commun. 9 (2007) 1530–1535.
[32] Z.H. Wen, Q. Wang, Q. Zhang, J.H. Li, Adv. Funct. Mater. 17 (2007) 2772–2778.
[33] H. Shibata, T. Morita, T. Ogura, K. Nishio, H. Sakai, M. Abe, M. Matsumoto, J. Mater. Sci. 44 (2009) 2541–2547.
[34] S.Y. Chen, L.Y. Jang, S. Cheng, J. Phys. Chem. B 110 (2006) 11761–11771.
[35] X. Xia, R. Oldman, R. Catlow, Chem. Mater. 21 (2009) 3576–3585.
[36] T.Y. Luo, T.X. Liang, C.S. Li, Mater. Sci. Eng. A 366 (2004) 206–209.
[37] T.Y. Luo, T.X. Liang, C.S. Li, Powder Technol. 139 (2004) 118–122.